Active Microwave Thermography for Detection of Lymphedema

by N. Agah*, F. Spano*, D. Fehr*,
K. Donnell**, M. Bonmarin*

* *ZHAW, Zurich University of Applied Sciences, Institute of Computational Physics, 8400, Winterthur, Switzerland*

** *Missouri University of Science and Technology, Microwave Sensing (μSense) Laboratory, Department of Electrical and Computer Engineering, Rolla, MO, USA*

Abstract

Lymphedema, a chronic disorder causing accumulation of interstitial fluid in soft tissues, lacks a diagnostic method combining non-invasiveness, portability, and depth sensitivity. This paper investigates Active Microwave Thermography (AMT) as a proof-of-concept for detecting fluid accumulation in PDMS-based tissue-mimicking phantoms with aqueous inclusions of varying salinity (0–25% NaCl w/v) and spatial distribution, embedded 5 mm below the inspection surface. Lock-in thermography measurements at R- and S-band frequencies (1.7–3.95 GHz) demonstrate that the thermal response scales with ionic concentration, confirming AMT sensitivity to subsurface fluid dielectric contrast.

1. Introduction

Lymphedema is a chronic disorder of the lymphatic system resulting from impaired lymphatic drainage, leading to the progressive accumulation of protein-rich interstitial fluid in soft tissues [1]. Although it most commonly arises as a secondary complication of oncological interventions, it may also stem from infections, trauma, or congenital malformations. Early and reliable detection is essential, as clinical signs typically manifest at advanced disease stages. Current diagnostic modalities — including lymphoscintigraphy [2], ICG fluorescence lymphography [3], magnetic resonance lymphangiography [4], and bioimpedance spectroscopy [5, 6] — each present significant trade-offs in terms of invasiveness, cost, accessibility, or sensitivity, revealing a persistent clinical need for a non-invasive, portable, and depth-sensitive diagnostic approach.

Active Microwave Thermography (AMT) is a promising candidate to address this gap. Originally developed for nondestructive testing (NDT) in civil and aerospace engineering [7–10], AMT induces localized heating through the selective absorption of high-frequency, non-ionizing electromagnetic (EM) energy by materials with high dielectric loss. The premise behind AMT has a foundation in thermography, a well-established NDT and medical imaging technique [11]. The heat, Q, induced during an AMT inspection is given by $Q = 2\pi f \varepsilon_0 \varepsilon_r'' E_{RMS}^2$, where f is the excitation frequency, ε_0 is the permittivity of free space, ε_r'' is the material's (dielectric) loss factor, and E_{RMS} is the local root mean square (RMS) electric field amplitude. The loss factor of aqueous biological fluids [12] is substantially greater than that of surrounding tissue at R- and S-band frequencies (1.7-2.6 and 2.6–3.95 GHz, respectively), a dielectric contrast already utilized for water ingress detection in rubber materials [13]. As such, AMT offers a non-invasive, label-free, and portable modality that is well suited for early detection of the subcutaneous fluid accumulation that is characteristic of lymphedema.

This paper presents a proof-of-concept study in which AMT is applied to PDMS-based tissue-mimicking phantoms containing aqueous inclusions of controlled salinity and volume. As the dielectric properties of the phantom material are important as it relates thermal generation in the phantom and the inclusion, the dielectric properties of the phantom material was characterized across both frequency bands, and preliminary thermal imaging results of the phantoms are reported.

2. Materials and Methods

2.1. Fabrication of the skin models mimicking the lymphedema tissues

PDMS was selected as the phantom matrix due to its similar characteristics to human skin. Several salinities (deionized water and NaCl solutions at 5, 10, 15, 20, and 25% w/v) were investigated for a single 270 μL inclusion at a depth of 5 mm from the imaged surface, representative of subcutaneous lymphedema fluid. While the salinity range exceeds physiological levels (~1% w/v), at this stage, it serves to control the dielectric loss factor rather than replicate fluid composition. Phantoms were cast from SYLGARD 184 PDMS (10:1 ratio), degassed, and poured into 3D-printed PETG molds (35 × 35 × 13 mm) in two layers cured at 70 °C for 4 h each. Aqueous inclusions were pipetted onto the first cured layer before the second layer was added and cured.

2.2. Dielectric Characterization

As the loss factor of the material is critically important as it relates to the potential for thermal generation via absorbed electromagnetic energy, dielectric characterization of polydimethylsiloxane (PDMS) was needed. To this end, a set of samples were cast with cross sections corresponding to S-band (2.6 – 3.95 GHz) and R-band (1.7 – 2.6 GHz) waveguide dimensions. Measurements were made by placing each sample inside a rectangular waveguide specimen holder of length 3.451 cm and 2.544 cm for R- and S-Band, respectively. The filled transmission line technique [14] was used for measurement. To do this, the sample holder was connected to two calibrated ports of an Anritsu MS4644A vector network analyzer (VNA). Then, the complex reflection and transmission properties were measured over both frequency bands. Using this measured data, the relative dielectric properties, ε_r, were calculated using the Nicolson-Ross-Weir/Baker Jarvis (NRW/Baker-Jarvis) procedure [14]. The results are provided in Table 1. As can be seen, the material is very low loss at R- and S-band frequencies, meaning that it will not heat when under high frequency illumination.

Table 1. Measured Complex Relative Permittivity ε_r

	S-Band		R-band		
Sample	1	2	3	4	5
Size	10.2 mm	7.7 mm	19.13 mm	15.19 mm	18.22 mm
Relative Permittivity	2.8 – j0.04	2.7 – j0.04	2.8 – j0.01	2.8 – j0.02	2.9 – j0.001

3. Thermal Measurements

The surface temperature of the phantoms was recorded with an Optris PI 640i infrared camera (640 × 480 px) positioned 30 cm from the phantom surface. The microwave excitation was generated by combined RF source and amplifier (RFS-2G42G5050(X)+, Mini-Circuits, Melville, NY) and delivered via a standard gain horn antenna placed 28 cm from the sample. Lock-in thermography was applied to enhance sensitivity: the RF excitation was square-wave modulated at 0.05 Hz (50% duty cycle, 30 W incident power) over 20 periods, and amplitude images were reconstructed using the Winterthur Instruments Tracer Lock-in Module (v1.2). The results of the thermal inspection are shown in Fig. 1.

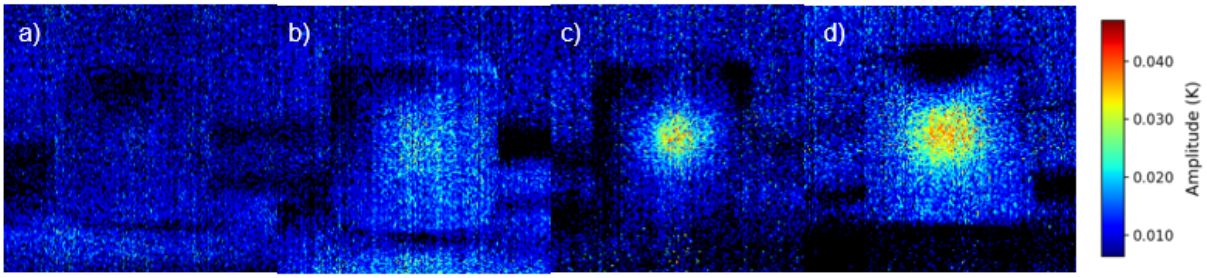

Fig. 1. Amplitude images of water droplets in PDMS across increasing salt concentrations. **a**–**d**, A single 270 µL inclusion at increasing salt concentration (w/v): **a**, blank; **b**, 5%; **c**, 15%; **d**, 25%.

4. Conclusion

This study presented a proof-of-concept investigation of Active Microwave Thermography (AMT) as a non-invasive diagnostic modality for the detection of interstitial fluid accumulation in lymphedema. PDMS-based tissue-mimicking phantoms with aqueous inclusions of controlled salinity were fabricated and characterized dielectrically, confirming PDMS as a suitable low-loss background matrix at R- and S-band frequencies. Lock-in thermography measurements demonstrated that the thermal signature of inclusions embedded 5 mm below the surface is detectable at the phantom surface and scales monotonically with ionic concentration, validating the sensitivity of AMT to subsurface fluid dielectric contrast. These results establish the physical basis for AMT as a non-invasive, non-contact, and portable alternative to existing lymphedema diagnostic tools, without the need for contrast agents or ionizing radiation.

Acknowledgements

This work was supported by the Swiss National Science Foundation (SNSF) under the Scientific Exchanges grant scheme (grant no. IZSEZ0_238337).

References

[1] A. K. Greene and J. A. Goss, "Diagnosis and management of lymphedema," *JAMA,* vol. 319, no. 13, pp. 1317-1318, 2018, doi: 10.1001/jama.2018.0246.

[2] A. Szuba and S. G. Rockson, "Lymphedema: Classification, diagnosis and therapy," *Vascular Medicine,* vol. 3, no. 2, pp. 145-156, 1998, doi: 10.1177/1358836X9800300208.

[3] N. Unno *et al.*, "A novel method of measuring human lymphatic pumping using indocyanine green fluorescence lymphography," *Journal of Vascular Surgery,* vol. 45, no. 6, pp. 1246-1252, 2007, doi: 10.1016/j.jvs.2007.02.043.

[4] N. F. Liu, Q. Lu, Z. H. Jiang, C. G. Wang, and J. G. Zhou, "Anatomic and functional evaluation of lymphatics in lymphedema patients with magnetic resonance lymphangiography," *Journal of Vascular Surgery,* vol. 49, no. 4, pp. 980-987, 2009, doi: 10.1016/j.jvs.2008.11.045.

[5] E. S. Qin, M. J. Bowen, S. L. James, and W. F. Chen, "Diagnostic accuracy of bioimpedance spectroscopy in patients with lymphedema: A retrospective cohort analysis," *Journal of Plastic, Reconstructive & Aesthetic Surgery,* vol. 71, no. 7, pp. 1041-1050, 2018, doi: 10.1016/j.bjps.2018.02.012.

[6] J. Spitz, A. Chao, D. Peterson, V. Subramaniam, S. Prakash, and R. Skoracki, "Bioimpedance Spectroscopy Is Not Associated With A Clinical Diagnosis of Breast Cancer-Related Lymphedema," *Lymphology,* vol. 52, pp. 134-142, 2019.

[7] A. Foudazi, M. T. Ghasr, and K. M. Donnell, "Characterization of Corroded Reinforced Steel Bars by Active Microwave Thermography," *IEEE Transactions on Instrumentation and Measurement,* vol. 64, no. 9, pp. 2583-2585, 2015, doi: 10.1109/tim.2015.2450353.

[8] A. Foudazi, C. A. Edwards, M. T. Ghasr, and K. M. Donnell, "Active Microwave Thermography for Defect Detection of CFRP-Strengthened Cement-Based Materials," *IEEE Transactions on Instrumentation and Measurement,* vol. 65, no. 11, pp. 2612-2620, 2016, doi: 10.1109/TIM.2016.2596080.

[9] A. Foudazi, I. Mehdipour, K. Donnell, and K. Khayat, "Evaluation of steel fiber distribution in cement-based mortars using active microwave thermography," *Materials and Structures,* vol. 49, no. 12, pp. 5051-5065, 2016, doi: 10.1617/s11527-016-0843-3.

[10] H. Zhang, R. Yang, Y. He, A. Foudazi, L. Cheng, and G. Tian, "A Review of Microwave Thermography Nondestructive Testing and Evaluation," *Sensors,* vol. 17, no. 5, 2017, doi: 10.3390/s17051123.

[11] S. Shepard, J. Lhota, B. Rubadeux, D. Wang, and T. Ahmed, "Reconstruction and enhancement of active thermographic image sequences," *Optical Engineering,* vol. 42, no. 5, pp. 1337-1342, 2003, doi: 10.1117/1.1566969.

[12] W. Liu, Y. Cao, X. Zhou, and D. Han, "Interstitial Fluid Behavior and Diseases," (in English), *Advanced Science,* Review vol. 9, no. 6, FEB 2022, Art no. ARTN 2100617, doi: 10.1002/advs.202100617.

[13] A. Mirala, A. Foudazi, M. Al Qaseer, and K. Donnell, "Active Microwave Thermography to Detect and Locate Water Ingress," *IEEE Transactions on Instrumentation and Measurement,* vol. 69, no. 12, pp. 9774-9783, 2020, doi: 10.1109/TIM.2020.3003394.

[14] K. J. Bois, L. F. Handjojo, A. D. Benally, K. Mubarak, and R. Zoughi, "Dielectric plug-loaded two-port transmission line measurement technique for dielectric property characterization of granular and liquid materials," *IEEE Transactions on Instrumentation and Measurement,* vol. 48, no. 6, pp. 1141-1148, 1999.